ARTICLES

CCR3 is a target for age-related macular degeneration diagnosis and therapy

Atsunobu Takeda[1]*, Judit Z. Baffi[1]*, Mark E. Kleinman[1]*, Won Gil Cho[1]*, Miho Nozaki[1,3], Kiyoshi Yamada[1], Hiroki Kaneko[1], Romulo J. C. Albuquerque[1,2], Sami Dridi[1], Kuniharu Saito[1], Brian J. Raisler[1,2], Steven J. Budd[4], Pete Geisen[4], Ariel Munitz[5], Balamurali K. Ambati[6,7], Martha G. Green[1], Tatsuro Ishibashi[8], John D. Wright[4], Alison A. Humbles[9]†, Craig J. Gerard[9], Yuichiro Ogura[3], Yuzhen Pan[10], Justine R. Smith[10], Salvatore Grisanti[11], M. Elizabeth Hartnett[4], Marc E. Rothenberg[5] & Jayakrishna Ambati[1,2]

Age-related macular degeneration (AMD), a leading cause of blindness worldwide, is as prevalent as cancer in industrialized nations. Most blindness in AMD results from invasion of the retina by choroidal neovascularisation (CNV). Here we show that the eosinophil/mast cell chemokine receptor CCR3 is specifically expressed in choroidal neovascular endothelial cells in humans with AMD, and that despite the expression of its ligands eotaxin-1, -2 and -3, neither eosinophils nor mast cells are present in human CNV. Genetic or pharmacological targeting of CCR3 or eotaxins inhibited injury-induced CNV in mice. CNV suppression by CCR3 blockade was due to direct inhibition of endothelial cell proliferation, and was uncoupled from inflammation because it occurred in mice lacking eosinophils or mast cells, and was independent of macrophage and neutrophil recruitment. CCR3 blockade was more effective at reducing CNV than vascular endothelial growth factor A (VEGF-A) neutralization, which is in clinical use at present, and, unlike VEGF-A blockade, is not toxic to the mouse retina. *In vivo* imaging with CCR3-targeting quantum dots located spontaneous CNV invisible to standard fluorescein angiography in mice before retinal invasion. CCR3 targeting might reduce vision loss due to AMD through early detection and therapeutic angioinhibition.

AMD affects 30–50 million people globally, with approximately 90% of severe vision loss attributed to CNV[1]. The worldwide prevalence of CNV is expected to double in the next decade owing to population ageing. Targeting the pro-angiogenic cytokine VEGF-A has been validated in patients with CNV[2–4]. However, substantial improvement of vision only occurs in one-third of patients treated with VEGF-A antagonists, and one-sixth of treated patients still progress to legal blindness. Moreover, safety concerns about the continual blockade of VEGF-A, which is constitutively expressed in the normal adult human retina[5], are emerging[6,7]. Thus, treatment strategies on the basis of more specific targeting of CNV are desirable. However, no molecular marker specific for human CNV has yet been reported.

CCR3 expression restricted to CNV in human eyes

In our studies examining the role of chemokines in angiogenesis, we discovered that CCR3 (also known as CD193)—a chemokine receptor best known for its role in promoting eosinophil and mast cell trafficking[8]—was expressed in human choroidal endothelial cells (CECs) only in the context of CNV due to AMD, and not in other non-proliferating or proliferating choroidal vasculature (Fig. 1). Immunolocalization studies showed that CCR3 was expressed in CECs of all examined specimens of surgically excised choroidal neovascular tissue from patients with AMD (18 out of 18) who had not received prior AMD treatment (Fig. 1a, b and Supplementary Fig. 1). In contrast, CCR3 was not expressed in CECs in the choroid of any patients with early (atrophic) AMD (0 out of 10), or in age-matched patients without AMD (0 out of 10) (Fig. 1c, d). CCR3 was also not immunolocalized in surgically excised tissue from patients with epiretinal fibrotic membranes (0 out of 6), or in CECs in patients with choroidal melanoma (0 out of 8) (Fig. 1e, f). Collectively, these data point to a highly specific pattern of CCR3 expression ($P = 7 \times 10^{-14}$, exact contingency table test) in CECs in neovascular AMD. Furthermore, we identified the expression of the CCR3 ligands eotaxin-1 (also known as CCL11), -2 (CCL24), and -3 (CCL26) in all examined specimens of surgically excised choroidal neovascular tissue from patients with AMD who had not received previous AMD treatment (Fig. 1g–j), suggesting that the eotaxin–CCR3 axis could be involved in this disease state. Notably, despite the abundance of eotaxins, eosinophils and mast cells were not identified in human CNV (Supplementary Fig. 2), consistent with earlier findings[9].

CCR3 stimulation promotes CEC migration and proliferation

The best determined pathological function of CCR3 so far has been its role in allergic diseases, such as asthma[10–14] and eosinophilic esophagitis[15]. There is a single report of its direct role in angiogenesis[16]. Although eosinophils and mast cells have been reported to be

[1]Department of Ophthalmology & Visual Science, [2]Department of Physiology, University of Kentucky, Lexington, Kentucky 40506, USA. [3]Department of Ophthalmology and Visual Science, Nagoya City University Graduate School of Medical Sciences, Nagoya 467-8601, Japan. [4]Department of Ophthalmology, The University of North Carolina at Chapel Hill, Chapel Hill, North Carolina 27599, USA. [5]Division of Allergy and Immunology, Department of Pediatrics, Cincinnati Children's Hospital Medical Center, University of Cincinnati, Cincinnati, Ohio 45229, USA. [6]Department of Ophthalmology and Visual Sciences, Moran Eye Center, University of Utah School of Medicine, Salt Lake City, Utah 84132, USA. [7]Department of Ophthalmology, Veterans Affairs Salt Lake City Healthcare System, Salt Lake City, Utah 84148, USA. [8]Department of Ophthalmology, Graduate School of Medical Sciences, Kyushu University, Fukuoka 812-8582, Japan. [9]Department of Medicine, Children's Hospital, Harvard Medical School, Boston, Massachusetts 02215, USA. [10]Casey Eye Institute, Oregon Health and Science University, Portland, Oregon 97239, USA. [11]Department of Ophthalmology, University of Luebeck, D-23538 Lübeck, Germany. †Present address: Respiratory, Inflammation and Autoimmunity, Medimmune, Inc., Gaithersburg, Maryland 20878, USA.
*These authors contributed equally to this work.

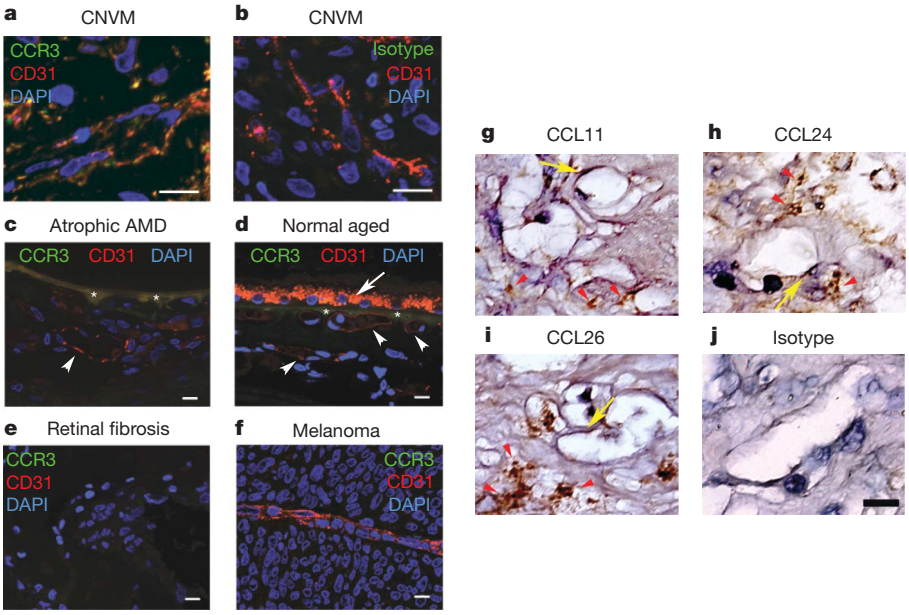

Figure 1 | CCR3 and eotaxins are expressed in CNV. **a**, **b**, Immunofluorescence shows that CCR3-receptor expression (green) colocalizes with $CD31^+$-expressing (red) blood vessels in surgically excised human AMD choroidal neovascular tissue (CNVM). Nuclei were stained blue with 4,6-diamidino-2-phenylindole (DAPI). The specificity of CCR3 staining in **a** is confirmed by the absence of staining with an isotype control IgG (green) in **b**. Individual red and green fluorescence channels are shown in Supplementary Fig. 1. **c**, **d**, CCR3 is not immunolocalized in $CD31^+$ (red) blood vessels (white arrowheads) in the choroid of patients with atrophic AMD who do not have CNV (**c**), or in aged patients without AMD (**d**). Autofluorescence of RPE (white arrow) and Bruch's membrane (asterisks) overlying choroid are seen. **e**, **f**, CCR3 is not expressed in surgically excised avascular retinal fibrosis tissue (**e**) or in the blood vessel of choroidal melanoma (**f**). **g**–**j**, Immunohistochemistry (golden brown reaction product) shows expression of CCL11 (**g**), CCL24 (**h**), and CCL26 (**i**) in surgically excised AMD choroidal neovascular tissue, primarily in the stroma (red arrowheads) but also in the blood vessels (yellow arrows). The specificity of staining is confirmed by the absence of staining with isotype control IgG (**j**). Scale bars, 10 μm.

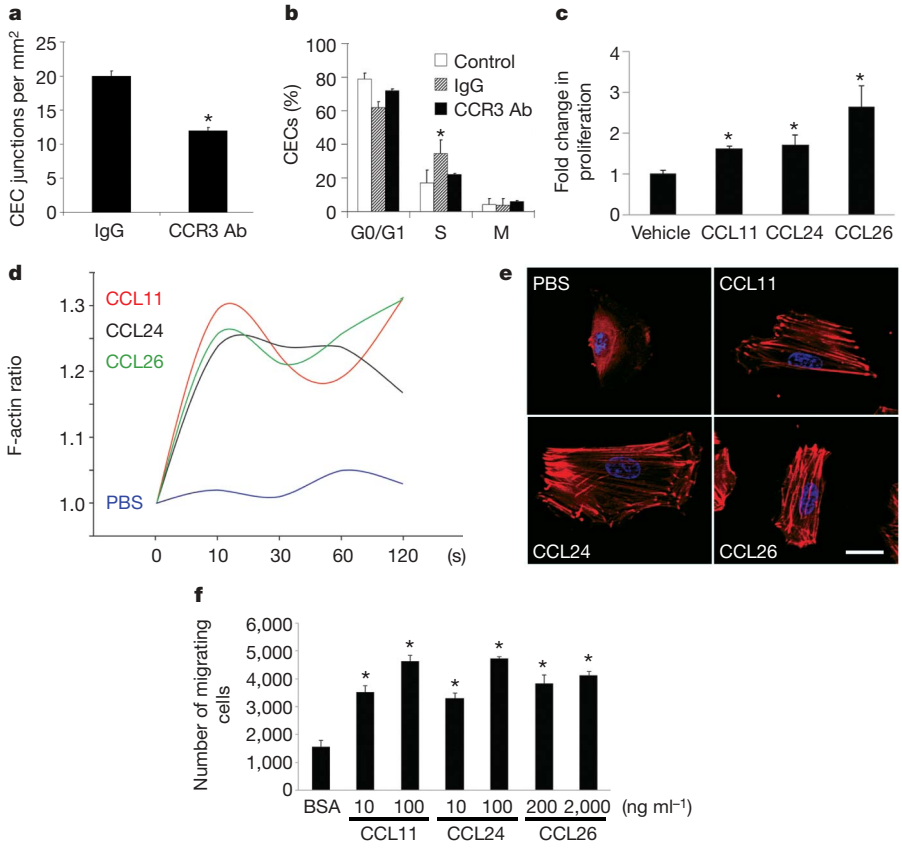

Figure 2 | CCR3 activation promotes angiogenesis. **a**, Tube formation of primary human CECs in Matrigel *in vitro* was reduced by neutralizing anti-human CCR3 antibodies (CCR3 Ab) compared to isotype IgG. $n = 6$, $^*P < 0.05$ compared to isotype IgG. **b**, Fraction of $CD31^+$ $VEGFR2^+$-gated mouse CECs *in vivo* in the proliferative state (S phase) was increased 5 days after laser injury in wild-type mouse eyes compared to control (uninjured eyes), and was reduced by intraocular administration of neutralizing anti-mouse CCR3 antibody compared to isotype IgG. $n = 6$–10, $^*P < 0.05$ compared to IgG treatment. **c**, Stimulation with eotaxins for 24 h induced human CEC proliferation. $n = 4$, $^*P < 0.05$ compared to BSA treatment. **d**, **e**, Stimulation with eotaxins, but not with PBS, induced actin polymerization in human CECs. The relative F-actin content is expressed as the ratio of the mean channel fluorescence between eotaxin-stimulated and media-alone-stimulated cells (**d**). Rhodamine–phalloidin staining (red) shows F-actin fibre formation in eotaxin-stimulated cells (**e**). Nuclei were stained blue with DAPI. Data representative of 3–4 independent experiments are shown. In **c** and **e**, 10 ng ml^{-1} CCL11, 100 ng ml^{-1} CCL24 and 2 μg ml^{-1} CCL26 were used. Scale bar, 20 μm. **f**, Stimulation with eotaxins for 16 h induces dose-dependent migration of human CECs across 8-μm pore size Transwells. $n = 5$–10, $^*P < 0.05$ compared to BSA treatment. Statistical significance was determined by Mann–Whitney U test (**a**–**c**, **f**); error bars depict s.e.m.

involved in angiogenesis[17,18], such actions are considered minor or isolated. Therefore, we studied the effects of CCR3 modulation on angiogenesis *in vitro* and *in vivo*. Neutralizing anti-CCR3 antibodies inhibited the tube formation of primary human CECs cultured in Matrigel *in vitro* (Fig. 2a). In an experimental model of CNV induced by laser injury in wild-type mice[19–24], neutralizing anti-CCR3 antibodies reduced the fraction of CECs *in vivo* that was in the proliferative state of the cell cycle (Fig. 2b). Consistent with this finding, each of the three eotaxins stimulated human CEC proliferation (Fig. 2c). Cytoskeletal rearrangement through polymerization of monomeric actin to microfilamentous F-actin, which is essential for eosinophil chemotaxis induced by the eotaxins, is also critical in angiogenic migration of endothelial cells. Stimulation of human CECs with any of the three eotaxins induced a rapid polymerization of actin molecules (Fig. 2d, e). All three eotaxins also activated RAC1 (Supplementary Fig. 3), a small GTPase that is critical in regulating endothelial cell spreading and migration, and promoted human CEC migration in a dose-dependent fashion (Fig. 2f). Collectively, these data demonstrate that CCR3 activation can promote several steps of angiogenesis. The expression of CCR3 on CECs *in vivo* is confined to choroidal neovascular tissues; however, *in vitro*, human CECs responded to CCR3 ligands. This might be owing to the presence of several CNV-promoting growth factors in the culture medium.

CCR3 receptor or ligand antagonism inhibits CNV

We studied the *in vivo* effects of CCR3 targeting in a mouse model of CNV induced by laser injury[22], which is the most widely used animal model of this disease. A single intraocular administration of either CCR3-neutralizing antibodies or a small molecule CCR3 receptor antagonist ((*S*)-methyl-2-naphthoylamino-3-(4-nitrophenyl)propionate; SB328437) suppressed laser-injury-induced CNV in wild-type mice in a dose-dependent fashion (Fig. 3a–c). CNV was also diminished in $Ccr3^{-/-}$ mice[25] compared to wild-type mice (Fig. 3d). The specificity of pharmacological CCR3 blockade was confirmed by demonstrating that CNV was not reduced in $Ccr3^{-/-}$ mice by CCR3-neutralizing antibodies or a CCR3 receptor antagonist ($116 \pm 7\%$ and $109 \pm 16\%$ of control, respectively; $n = 5$; $P > 0.1$). CCL11 and CCL24, the principal mouse ligands for CCR3, were markedly increased soon after laser injury, and immunolocalized to the retinal pigmented epithelium (RPE), which is adjacent to CECs (Fig. 3e, f).

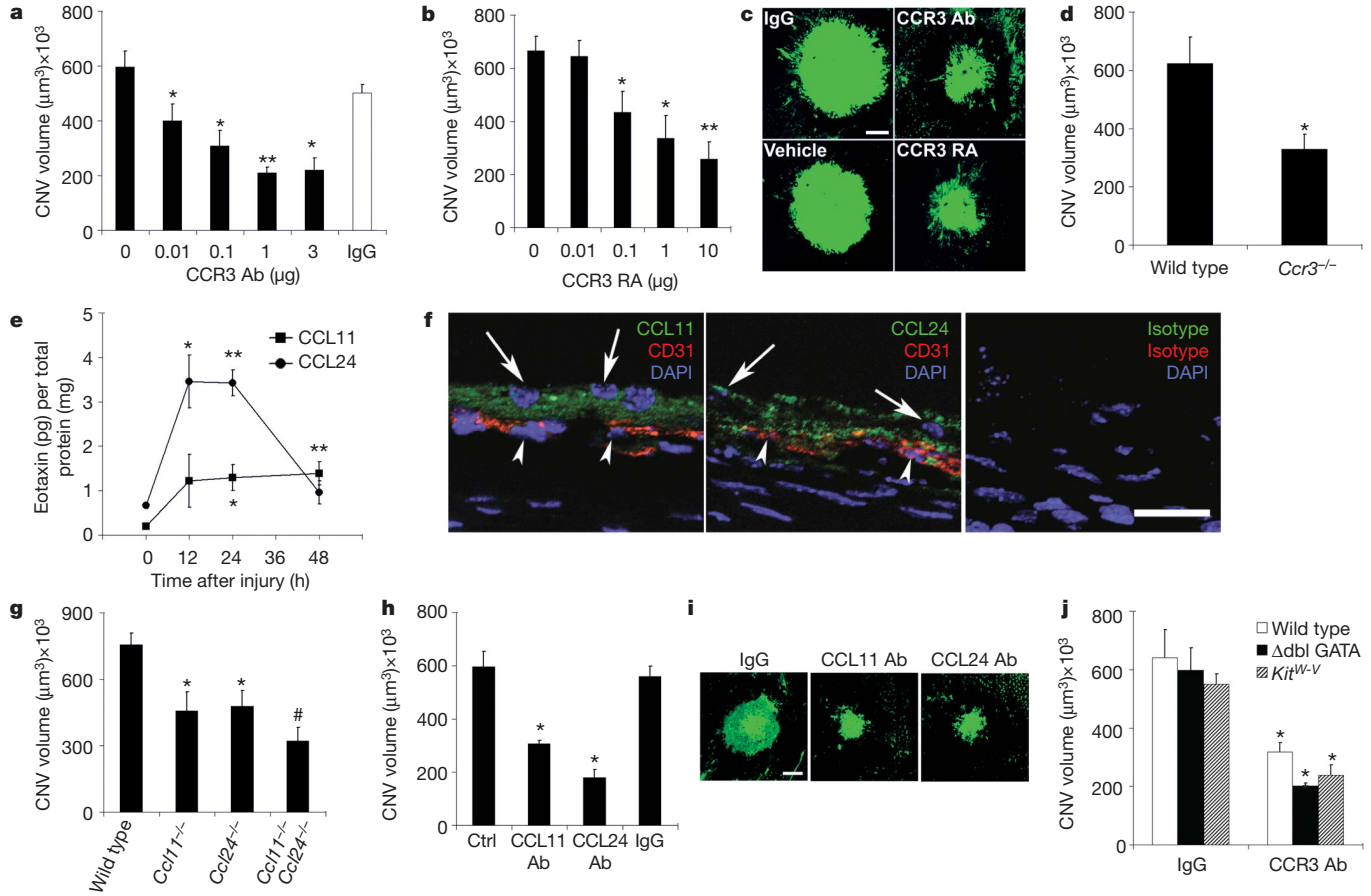

Figure 3 | CNV reduced by CCR3 or eotaxin ablation or blockade independent of leukocyte modulation. **a**, **b**, Laser-induced CNV in wild-type mice was reduced by neutralizing anti-mouse CCR3 antibody (CCR3 Ab) compared to isotype IgG (**a**) and by the CCR3 receptor antagonist (RA) SB328437 compared to vehicle (PBS/DMSO) (**b**) in a dose-dependent fashion. $n = 8$–12, $^*P < 0.05$, $^{**}P < 0.01$ compared to no antibody or receptor antagonist. **c**, Representative examples of CNV in drug-treated mice. **d**, Laser-induced CNV was reduced in $Ccr3^{-/-}$ mice compared to wild-type mice. $n = 9$, $^*P < 0.05$ compared to wild-type mice. **e**, Eotaxin-1 (CCL11) and eotaxin-2 (CCL24) protein levels, measured by ELISA, were increased after laser injury in wild-type mice. $n = 6$, $^*P < 0.05$ and $^{**}P < 0.01$ compared to the 0 h baseline. **f**, CCL11 and CCL24 immunofluorescence (green) was localized in the RPE cell layer (arrows) adjacent to $CD31^+$ (red) CECs (arrowheads) on day 1 after laser injury in wild-type mice. Nuclei were stained blue by DAPI. No specific immunofluorescence was detected with isotype control IgGs. Images representative of three independent experiments are shown. **g**, Laser-induced CNV was reduced in $Ccl11^{-/-}$ and $Ccl24^{-/-}$ mice compared to wild-type mice. $n = 8$–10, $^*P < 0.05$ compared to wild-type mice. CNV is further reduced in $Ccl11^{-/-}$ $Ccl24^{-/-}$ mice compared to single-null mice. $\#P < 0.05$ compared to single-null mice. **h**, Laser-induced CNV in wild-type mice was reduced by neutralizing antibodies against mouse CCL11 or CCL24 compared to isotype IgG. $n = 7$–10, $^*P < 0.05$ compared to no injection (control; Ctrl) or IgG. **i**, Representative examples of CNV in eotaxin-neutralized mice. **j**, Neutralizing anti-CCR3 antibodies reduced laser-induced CNV in mice deficient in eosinophils (ΔdblGATA) or mast cells ($Kit^{W\text{-}v}$). $n = 6$–9, $^*P < 0.05$ compared to IgG. Scale bars, 100 μm (**c**, **i**), and 20 μm (**f**). Error bars depict s.e.m.

Also, human RPE cells synthesized all three eotaxins (Supplementary Fig. 4), implicating these cells, which are abundantly interspersed in CNV[9], as a source of CCR3 ligands in CNV. Genetic ablation of either *Ccl11* (ref. 26) or *Ccl24* (ref. 12) reduced CNV, whereas the neovascular response in *Ccl11*$^{-/-}$ *Ccl24*$^{-/-}$ mice[12] was suppressed to a greater extent than in either of the single knockout mice, suggesting cooperation between these two ligands in this system (Fig. 3g). A single intraocular administration of neutralizing antibodies against CCL11 or CCL24 also suppressed CNV in wild-type mice (Fig. 3h, i), validating these CCR3 ligands as anti-angiogenic targets. Together, these data demonstrate that CCR3 activation is essential for *in vivo* angiogenesis in the most widely used preclinical model of neovascular AMD.

CCR3-driven angiogenesis uncoupled from inflammation

We sought to determine whether CCR3 targeting reduced CNV solely by anti-angiogenic mechanisms, or whether anti-inflammatory mechanisms were also involved. Neither eosinophils nor mast cells (defined as CCR3^{hi}CD3^{-}CD117^{int}CD49d^{+} and CCR3^{int}CD3^{-}CD117^{hi}CD49d^{+} cells, respectively) were recruited to the choroid after laser injury, as monitored by flow cytometry (Supplementary Fig. 5). Furthermore, the CNV response in eosinophil-deficient ΔdblGATA mice[11] (containing a deletion of the double GATA site) and mast-cell-deficient *Kit*$^{W\text{-}v}$/*Kit*$^{W\text{-}v}$ mice[27] was not different from the response in wild-type mice (Fig. 3j). Moreover, intraocular administration of neutralizing anti-CCR3 antibodies reduced CNV in ΔdblGATA or *Kit*$^{W\text{-}v}$/*Kit*$^{W\text{-}v}$ mice to the same extent as in wild-type mice. Thus, although eosinophils and mast cells have been reported to be capable of driving angiogenesis in other systems[17,18], both cell types are dispensable in the development of experimental CNV. Although neutrophil and macrophage infiltration are crucial for the development of experimental CNV[23,28], CCR3-receptor targeting did not affect recruitment of either inflammatory cell type (defined as Gr-1^{+}F4/80^{-} and F4/80^{+}CD11c^{-} cells, respectively; Supplementary Fig. 5). Therefore, the angioinhibitory effect of CCR3 blockade in this model is a direct anti-vascular effect, and does not seem to involve modulation of cellular inflammation. The mechanisms underlying the paucity of eosinophils and mast cells in CNV remain to be defined. One potential explanation could be the expression of CXCL9 in CNV, which blocks eotaxin-induced CCR3-mediated eosinophil recruitment (Supplementary Fig. 6)[29,30]. Other mechanisms influencing adhesion or mobilization of these leukocytes might also be operative.

CNV bioimaging by CCR3 targeting

Because invasion of the retina by CNV results in morphological and functional disruption of the retina, early detection of CNV is desirable; indeed, detection of CNV before retinal invasion would be ideal. CNV that has breached the retina can be detected by fluorescein angiography. However, this diagnostic modality cannot detect CNV before it has invaded the retina, that is, when it is still limited to the choroid. Yet, post-mortem histopathological studies have shown that substantial numbers of patients in whom fluorescein angiography does not reveal the presence of CNV nevertheless have CNV that has not yet invaded the retina[31]. Therefore, we explored whether CCR3-targeted bioimaging using anti-CCR3 Fab antibody fragments (Supplementary Fig. 7) conjugated to quantum dots (QDot-CCR3 Fab) could detect CNV before it became clinically evident.

We previously described the spontaneous development of CNV in senescent mice deficient in monocyte chemoattractant protein-1 (CCL2, also known as MCP-1) or its CCR2 receptor[32]. Similar pathology occurs at a younger age in *Ccl2*$^{-/-}$ *Ccr2*$^{-/-}$ mice (J.A., M.E.K., J.Z.B., H.K. and B.J.R., unpublished data). These mice also undergo outer retinal degeneration rapidly (Supplementary Fig. 8). We tested whether fundus angiography after intravenous injection of QDot-CCR3 Fab could detect subretinal CNV in these mice. QDot-CCR3 Fab angiography demonstrated hyperfluorescent signals in regions of the fundus of these mice that were silent on fluorescein angiography (Fig. 4a, b). The specificity of CCR3 targeting was confirmed by the absence of hyperfluorescent signals in *Ccl2*$^{-/-}$ *Ccr2*$^{-/-}$ mice injected with QDot-isotype Fab, and in wild-type mice injected with QDot-CCR3 Fab (Fig. 4b and Supplementary Fig. 9). Histological examination of these areas showed proliferating (Ki67^{+}) CCR3^{+} blood vessels in the choroid that had not yet invaded the retina, along with the accumulation of QDot-CCR3 Fab in these vessels (Fig. 4c–g). These data provide proof-of-principle that CCR3-targeted bioimaging can detect subclinical CNV before it disrupts the retina and causes vision loss.

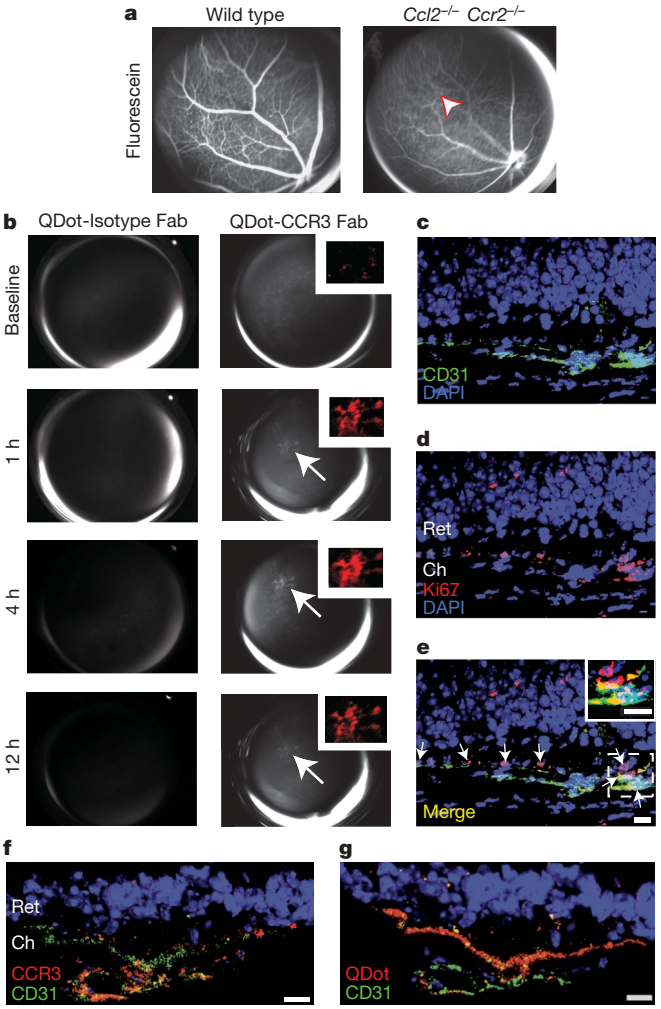

Figure 4 | CCR3-targeting quantum dots detect subretinal CNV. a, Images of the fundus taken after intravenous injection of sodium fluorescein in wild-type and *Ccl2*$^{-/-}$ *Ccr2*$^{-/-}$ mice show normal retinal vascular filling but no areas of hyperfluorescence indicative of CNV. **b**, After intravenous injection of QDot-CCR3 Fab in the same *Ccl2*$^{-/-}$ *Ccr2*$^{-/-}$ mouse shown in **a**, focal branching choroidal hyperfluorescence was visualized (arrow) at 1 h in the same area that was not hyperfluorescent during fluorescein angiography (arrowhead in **a**). The intensity of this hyperfluorescence (shown in red pseudocolour in the inset) increased, attaining a peak at 4 h, and then declined in intensity but still persisted at 12 h. Corresponding images of QDot-Isotype Fab angiography showed no hyperfluorescence. **c**–**e**, The region corresponding to the area of hyperfluorescence seen on QDot-CCR3 Fab angiography in **b** contained several CD31^{+} blood vessels in the choroid (Ch) that were proliferating (Ki67^{+}; arrows) and had not invaded the retina (Ret). Individual green (CD31^{+}, **c**), red (Ki67^{+}, **d**), and merged (**e**) fluorescence channel images are shown. Nuclei were stained with DAPI (blue). Arrows point to proliferating endothelial cells. The inset in **e** shows Ki67^{+} CD31^{+} cells in higher magnification. **f**, QDot-CCR3 Fab hyperfluorescent areas were localized to areas of subretinal CNV with CCR3^{+} endothelial cells. **g**, The QDot label was visualized within CD31^{+} vasculature of subretinal CNV lesions. Images are representative of six independent experiments. Scale bars, 10 μm (**c**–**g**).

CCR3 targeting is superior to VEGF-A targeting

By comparing CCR3 targeting to VEGF-A targeting, the most effective approved treatment for human CNV, we found that CCR3-neutralizing antibodies were more effective than VEGF-A-neutralizing antibodies ($68 \pm 3\%$ versus $57 \pm 4\%$) at inhibiting laser-induced CNV in mice (Supplementary Fig. 10). In the laser-injury model, CCR3 neutralization did not change VEGF-A levels in the RPE/choroid and VEGF-A blockade did not change CCR3 expression on CECs (Supplementary Fig. 11): these two pathways seem to not be directly coupled. Repeated intravitreous administration of anti-VEGF-A antibodies resulted in anatomical and functional damage to the retina in wild-type mice (Supplementary Fig. 12), consistent with earlier reports that anti-VEGF-A therapy induces dysfunction in and damage to the inner and outer murine retina[6,7]. These effects were modest at a dose of anti-VEGF-A antibodies that suppressed mouse CNV, but more pronounced at a higher dose that is comparable to the dose used in humans. It should be noted that anti-VEGF-A pharmacotherapy has not been associated with an increased risk of profound retinal damage in humans[33], but subtle abnormalities have been observed[34,35] and some adverse effects might be misattributed to disease progression. In contrast to VEGF-A blockade, neither an anti-CCR3 antibody nor a CCR3 receptor antagonist induced retinal toxicity in wild-type mice, as confirmed by fundus imaging and electrophysiological function (Supplementary Fig. 12). *Vegfa* deletion is embryonically lethal[36,37] and conditional ablation of *Vegfa* in the RPE induces profound retinal degeneration and visual dysfunction[38]. In contrast, the $Ccr3^{-/-}$ mouse retina was normal in appearance and electrophysiological function (Supplementary Fig. 13).

Discussion

Our findings suggest that CCR3 targeting may be a safe and viable strategy for early detection (using biocompatible quantum dots or other bioimaging fluorochromes, such as near infrared dyes) and treatment of CNV (by receptor or ligand targeting), and might be superior to the current standard of care. CCR3 bioimaging is probably most useful in individuals with RPE pigmentary disturbances and multiple subretinal lipoproteinaceous deposits known as drusen or fellow eye involvement with clinically evident CNV, as they are known to be at high risk for developing CNV[39,40]. Similar techniques might be useful in non-invasively bioimaging other metabolic or molecular markers to provide information about disease pathogenesis or activity.

Several strategies have yielded molecular markers that are preferentially expressed on proliferating endothelial cells such as those in tumour vasculature[41,42]; however, CCR3 has not been identified in any of these reports. Therefore, our studies identify CCR3 as a new marker of pathological angiogenesis and as a functional target in neovascular AMD. These findings should also prompt a search for genetic polymorphisms in the eotaxin–CCR3 axis in patients with AMD, and investigations of CCR3 function in other models of angiogenesis. Also, it is tempting to speculate that targeting CCR3 might provide dual benefits in asthma, which involves varying degrees of eosinophilic inflammation as well as angiogenic airway remodelling[43].

METHODS SUMMARY

Mouse model of CNV. Laser photocoagulation (OcuLight GL, Iridex Corporation) was performed on mouse eyes to induce CNV, and CNV volumes were measured 7 days after injury by scanning laser confocal microscopy (TCS SP, Leica), as previously described[22].

Drug injections. Rat IgG2a neutralizing antibody against mouse CCR3 (R&D Systems), control rat IgG2a (Serotec), goat neutralizing antibody against mouse CCL11 (R&D Systems), goat neutralizing antibody against mouse CCL24 (R&D Systems), control goat IgG (Jackson Immunoresearch), or (*S*)-methyl-2-naphthoylamino-3-(4-nitrophenyl)propionate (SB328437; Calbiochem) dissolved in dimethylsulphoxide (DMSO) were injected into the vitreous humour using a 33-gauge double-calibre needle (Ito Corporation) once, immediately after laser injury as previously described[22].

CCR3 bioimaging. Fab fragments were created from monoclonal IgG2a antibody raised against the extracellular domain of murine CCR3 (R&D Systems) and an isotype rat IgG2a (R&D Systems) using a commercially available papain-based kit (Pierce). Recovered fragments were conjugated with quantum dots (Invitrogen, QDot-800) and resuspended in sterile PBS. $Ccl2^{-/-}$ $Ccr2^{-/-}$ mice were administered 100 μg of tagged CCR3 Fab or isotype Fab by tail-vein injection after acquiring baseline fluorescent imaging using a Topcon retinal camera (TRC-50IX). Serial images were then acquired at 1, 4 and 12 h, after which eyes were collected and frozen in OCT for immunofluorescent analyses. Retinal images were analysed (ImageNet, Topcon) by comparison to baseline and fluorescein angiographic data. Hyperfluorescent areas were then cropped, equally thresholded, and pseudocoloured (Photoshop CS3, Adobe). Sections from QDot-conjugated CCR3 or rat IgG2a isotype Fab injected animals were fixed in 4% paraformaldehyde and blocked with 5% normal donkey serum/5% goat serum in PBS, stained with rat anti-mouse CD31 (BD Biosciences) and either rabbit anti-mouse CCR3 (Santa Cruz) or rabbit anti-Ki67 (Abcam), followed by appropriate fluorescent secondary antibodies (Alexa Fluor 488/594, Invitrogen), and evaluated by confocal laser scanning microscopy (Leica SP-5).

Full Methods and any associated references are available in the online version of the paper at www.nature.com/nature.

Received 22 March; accepted 21 May 2009.
Published online 14 June 2009.

1. Ambati, J., Ambati, B. K., Yoo, S. H., Ianchulev, S. & Adamis, A. P. Age–related macular degeneration: etiology, pathogenesis, and therapeutic strategies. *Surv. Ophthalmol.* **48,** 257–293 (2003).
2. Gragoudas, E. S., Adamis, A. P., Cunningham, E. T. Jr, Feinsod, M. & Guyer, D. R. Pegaptanib for neovascular age-related macular degeneration. *N. Engl. J. Med.* **351,** 2805–2816 (2004).
3. Brown, D. M. *et al.* Ranibizumab versus verteporfin for neovascular age-related macular degeneration. *N. Engl. J. Med.* **355,** 1432–1444 (2006).
4. Rosenfeld, P. J. *et al.* Ranibizumab for neovascular age-related macular degeneration. *N. Engl. J. Med.* **355,** 1419–1431 (2006).
5. Famiglietti, E. V. *et al.* Immunocytochemical localization of vascular endothelial growth factor in neurons and glial cells of human retina. *Brain Res.* **969,** 195–204 (2003).
6. Nishijima, K. *et al.* Vascular endothelial growth factor-A is a survival factor for retinal neurons and a critical neuroprotectant during the adaptive response to ischemic injury. *Am. J. Pathol.* **171,** 53–67 (2007).
7. Saint-Geniez, M. *et al.* Endogenous VEGF is required for visual function: evidence for a survival role on muller cells and photoreceptors. *PLoS One* **3,** e3554 (2008).
8. Rothenberg, M. E. & Hogan, S. P. The eosinophil. *Annu. Rev. Immunol.* **24,** 147–174 (2006).
9. Submacular Surgery Trials Research Group. Histopathologic and ultrastructural features of surgically excised subfoveal choroidal neovascular lesions: submacular surgery trials report no. 7. *Arch. Ophthalmol.* **123,** 914–921 (2005).
10. Justice, J. P. *et al.* Ablation of eosinophils leads to a reduction of allergen-induced pulmonary pathology. *Am. J. Physiol. Lung Cell. Mol. Physiol.* **284,** L169–L178 (2003).
11. Humbles, A. A. *et al.* A critical role for eosinophils in allergic airways remodeling. *Science* **305,** 1776–1779 (2004).
12. Pope, S. M., Zimmermann, N., Stringer, K. F., Karow, M. L. & Rothenberg, M. E. The eotaxin chemokines and CCR3 are fundamental regulators of allergen-induced pulmonary eosinophilia. *J. Immunol.* **175,** 5341–5350 (2005).
13. Jose, P. J. *et al.* Eotaxin: a potent eosinophil chemoattractant cytokine detected in a guinea pig model of allergic airways inflammation. *J. Exp. Med.* **179,** 881–887 (1994).
14. Teixeira, M. M. *et al.* Chemokine-induced eosinophil recruitment. Evidence of a role for endogenous eotaxin in an *in vivo* allergy model in mouse skin. *J. Clin. Invest.* **100,** 1657–1666 (1997).
15. Blanchard, C. *et al.* Eotaxin-3 and a uniquely conserved gene-expression profile in eosinophilic esophagitis. *J. Clin. Invest.* **116,** 536–547 (2006).
16. Salcedo, R. *et al.* Eotaxin (CCL11) induces *in vivo* angiogenic responses by human $CCR3^+$ endothelial cells. *J. Immunol.* **166,** 7571–7578 (2001).
17. Puxeddu, I. *et al.* Human peripheral blood eosinophils induce angiogenesis. *Int. J. Biochem. Cell Biol.* **37,** 628–636 (2005).
18. Heissig, B. *et al.* Low-dose irradiation promotes tissue revascularization through VEGF release from mast cells and MMP-9-mediated progenitor cell mobilization. *J. Exp. Med.* **202,** 739–750 (2005).
19. Tobe, T. *et al.* Targeted disruption of the FGF2 gene does not prevent choroidal neovascularization in a murine model. *Am. J. Pathol.* **153,** 1641–1646 (1998).
20. Nozaki, M. *et al.* Drusen complement components C3a and C5a promote choroidal neovascularization. *Proc. Natl Acad. Sci. USA* **103,** 2328–2333 (2006).
21. Nozaki, M. *et al.* Loss of SPARC-mediated VEGFR-1 suppression after injury reveals a novel antiangiogenic activity of VEGF-A. *J. Clin. Invest.* **116,** 422–429 (2006).
22. Kleinman, M. E. *et al.* Sequence- and target-independent angiogenesis suppression by siRNA via TLR3. *Nature* **452,** 591–597 (2008).

23. Sakurai, E., Anand, A., Ambati, B. K., van Rooijen, N. & Ambati, J. Macrophage depletion inhibits experimental choroidal neovascularization. *Invest. Ophthalmol. Vis. Sci.* **44,** 3578–3585 (2003).
24. Sakurai, E. *et al.* Targeted disruption of the CD18 or ICAM-1 gene inhibits choroidal neovascularization. *Invest. Ophthalmol. Vis. Sci.* **44,** 2743–2749 (2003).
25. Humbles, A. A. *et al.* The murine CCR3 receptor regulates both the role of eosinophils and mast cells in allergen-induced airway inflammation and hyperresponsiveness. *Proc. Natl Acad. Sci. USA* **99,** 1479–1484 (2002).
26. Rothenberg, M. E., MacLean, J. A., Pearlman, E., Luster, A. D. & Leder, P. Targeted disruption of the chemokine eotaxin partially reduces antigen-induced tissue eosinophilia. *J. Exp. Med.* **185,** 785–790 (1997).
27. Kitamura, Y., Go, S. & Hatanaka, K. Decrease of mast cells in W/W^v mice and their increase by bone marrow transplantation. *Blood* **52,** 447–452 (1978).
28. Zhou, J. *et al.* Neutrophils promote experimental choroidal neovascularization. *Mol. Vis.* **11,** 414–424 (2005).
29. Fulkerson, P. C. *et al.* Negative regulation of eosinophil recruitment to the lung by the chemokine monokine induced by IFN-γ (Mig, CXCL9). *Proc. Natl Acad. Sci. USA* **101,** 1987–1992 (2004).
30. Fulkerson, P. C., Zhu, H., Williams, D. A., Zimmermann, N. & Rothenberg, M. E. CXCL9 inhibits eosinophil responses by a CCR3- and Rac2-dependent mechanism. *Blood* **106,** 436–443 (2005).
31. Green, W. R. & Key, S. N. III. Senile macular degeneration: a histopathologic study. *Trans. Am. Ophthalmol. Soc.* **75,** 180–254 (1977).
32. Ambati, J. *et al.* An animal model of age-related macular degeneration in senescent Ccl-2- or Ccr-2-deficient mice. *Nature Med.* **9,** 1390–1397 (2003).
33. Ip, M. S. *et al.* Anti-vascular endothelial growth factor pharmacotherapy for age-related macular degeneration: a report by the American Academy of Ophthalmology. *Ophthalmology* **115,** 1837–1846 (2008).
34. Sayanagi, K., Sharma, S. & Kaiser, P. K. Photoreceptor status after anti-vascular endothelial growth factor therapy in exudative age-related macular degeneration. *Br. J. Ophthalmol.* **93,** 622–626 (2009).
35. Yodoi, Y. *et al.* Central retinal sensitivity after intravitreal injection of bevacizumab for myopic choroidal neovascularization. *Am. J. Ophthalmol.* **147,** 816–824 (2009).
36. Carmeliet, P. *et al.* Abnormal blood vessel development and lethality in embryos lacking a single VEGF allele. *Nature* **380,** 435–439 (1996).
37. Ferrara, N. *et al.* Heterozygous embryonic lethality induced by targeted inactivation of the VEGF gene. *Nature* **380,** 439–442 (1996).
38. Marneros, A. G. *et al.* Vascular endothelial growth factor expression in the retinal pigment epithelium is essential for choriocapillaris development and visual function. *Am. J. Pathol.* **167,** 1451–1459 (2005).
39. Bressler, S. B., Maguire, M. G., Bressler, N. M. & Fine, S. L. (The Macular Photocoagulation Study Group). Relationship of drusen and abnormalities of the retinal pigment epithelium to the prognosis of neovascular macular degeneration. *Arch. Ophthalmol.* **108,** 1442–1447 (1990).
40. Macular Photocoagulation Study Group. Risk factors for choroidal neovascularization in the second eye of patients with juxtafoveal or subfoveal choroidal neovascularization secondary to age-related macular degeneration. *Arch. Ophthalmol.* **115,** 741–747 (1997).
41. St Croix, B. *et al.* Genes expressed in human tumor endothelium. *Science* **289,** 1197–1202 (2000).
42. Zhang, L. *et al.* Gene expression profiles in normal and cancer cells. *Science* **276,** 1268–1272 (1997).
43. Wenzel, S. E. Eosinophils in asthma—closing the loop or opening the door? *N. Engl. J. Med.* **360,** 1026–1028 (2009).

Supplementary Information is linked to the online version of the paper at www.nature.com/nature.

Acknowledgements We thank R. King, L. Xu, M. McConnell, K. Emerson, G. R. Pattison and M. Mingler for technical assistance, J. M. Farber for the gift of a reagent, R. J. Kryscio for statistical guidance, and B. Appukuttan, M. W. Fannon, R. Mohan, A. P. Pearson, A. M. Rao, G. S. Rao and K. Ambati for discussions. J.A. was supported by National Eye Institute/National Institutes of Health (NIH) grants EY015422, EY018350 and EY018836, the Doris Duke Distinguished Clinical Scientist Award, the Burroughs Wellcome Fund Clinical Scientist Award in Translational Research, the Macula Vision Research Foundation, the E. Matilda Ziegler Foundation for the Blind, the Dr. E. Vernon Smith and Eloise C. Smith Macular Degeneration Endowed Chair, the Lew R. Wassermann Merit & Physician Scientist Awards (Research to Prevent Blindness, RPB), the American Health Assistance Foundation, and a departmental unrestricted grant from the RPB. J.Z.B. was supported by the University of Kentucky Physician Scientist Award. M.E.K. was supported by the International Retinal Research Foundation Dr. Charles Kelman Postdoctoral Scholar Award. R.J.C.A. was supported by Fight for Sight. B.K.A. was supported by NIH grants EY017182 and EY017950, the VA Merit Award and the Department of Defense. M.E.R. was supported by NIH grants AI45898 and DK076893. C.J.G. was supported by NIH grant AI039759. M.E.H. was supported by NIH grants EY017011 and EY015130 and a RPB departmental unrestricted grant. J.R.S. was supported by NIH grant EY010572, and RPB Career Development Award and a departmental unrestricted grant.

Author Contributions A.T., J.Z.B., M.E.K., W.G.C., M.N., K.Y., H.K., R.J.C.A., S.D., K.S., B.J.R., M.G.G., S.J.B., P.G. and A.M. performed experiments. S.G., A.A.H., Y.P., J.D.W., J.R.S., Y.O. and T.I. provided reagents. J.A. conceived and directed the project, and, with assistance from B.K.A., M.E.H., M.E.R., R.J.C.A. and J.R.S., wrote the paper. All authors had the opportunity to discuss the results and comment on the manuscript.

Author Information Reprints and permissions information is available at www.nature.com/reprints. The authors declare competing financial interests: details accompany the full-text HTML version of the paper at www.nature.com/nature. Correspondence and requests for materials should be addressed to J.A. (jamba2@email.uky.edu).

METHODS

Human tissue. Choroidal neovascular tissue was excised from patients with AMD who had no prior treatment for CNV. Retinal fibrosis tissue was excised from patients with a diagnosis of epiretinal membrane formation. Donor eyes from patients with atrophic AMD without CNV and patients without AMD were obtained from eye banks. Eyes with choroidal melanoma were obtained by surgical enucleation. The study followed the guidelines of the Declaration of Helsinki. Institutional review boards granted approval for allocation and histological analysis of specimens.

Animals. All animal experiments were in accordance with the guidelines of the University of Kentucky Institutional Animal Care and Use Committee and the Association for Research in Vision and Ophthalmology. C57BL/6J and $Kit^{W\text{-}v}$/$Kit^{W\text{-}v}$ mice were purchased from The Jackson Laboratory. $Ccr3^{-/-}$, $Ccl11^{-/-}$, $Ccl24^{-/-}$, $Ccl11^{-/-}$ $Ccl24^{-/-}$ and Δdbl GATA mice have been previously described[11,12,25,26]. $Ccl2^{-/-}$ $Ccr2^{-/-}$ mice were generated by interbreeding single knockout mice described previously[32].

Drug injections. Rat IgG2a neutralizing antibody against mouse CCR3 (R&D Systems), control rat IgG2a (Serotec), goat neutralizing antibody against mouse CCL11 (1 μg; R&D Systems), goat neutralizing antibody against mouse CCL24 (5 μg; R&D Systems), control goat IgG (Jackson Immunoresearch), or (*S*)-methyl-2-naphthoylamino-3-(4-nitrophenyl)propionate (SB328437; Calbiochem) dissolved in DMSO were injected into the vitreous humour of mice using a 33-gauge double-calibre needle (Ito Corporation) once, immediately after laser injury as previously described[22].

Flow cytometry. Rat antibody against mouse CCR3 (1:250; Santa Cruz) coupled with phycoerythrin (PE)-donkey antibody against rat IgG (1:250; Jackson Immunoresearch) or AlexaFluor647-conjugated rat antibody against mouse CCR3 (10 μg ml^{-1}; BD Biosciences) were used to quantify cell surface receptor expression on CECs, defined by CD31^{+} VEGFR-2^{+} expression, gated by FITC-conjugated rat antibody against mouse CD31 (20 μg ml^{-1}; BD Biosciences) and PE-conjugated rat antibody against mouse VEGFR-2 (20 μg ml^{-1}; BD Biosciences). Macrophages, neutrophils, eosinophils and mast cells were defined as F4/80^{+} CD11c^{-}, Gr-1^{+} F4/80^{-}, CCR3^{hi} CD3^{-} CD117^{int} CD49d^{+} and CCR3^{int} CD3^{-} CD117^{hi} CD49d^{+} cells, respectively. The DNA content for cell cycle was analysed after incubation with propidium iodide (0.05 mg ml^{-1}; Molecular Probes) containing 0.1% Triton X-100 and RNase A (0.1 mg ml^{-1}; Roche). Samples were analysed on a LSRII (Becton Dickinson).

Immunolabelling. Immunofluorescent staining was performed with antibodies against human CCR3 (rat monoclonal, R&D Systems) or human CD31 (mouse monoclonal, Dako), and identified with Alexa 488 (Molecular Probes) or Cy3 secondary antibodies (Jackson ImmunoResearch). Immunohistochemical staining with the primary antibodies specific for human eotaxins-1, -2 and -3 (mouse monoclonal, R&D Systems) was performed using horseradish peroxidase. Laser-injured mouse eye sections were stained with antibodies against mouse CCL11 or CCL24 (both R&D Systems) along with antibody against mouse CD31 (BD Biosciences) and visualized with FITC or Cy3 secondary antibodies. Images were obtained using Leica SP5 or Zeiss Axio Observer Z1 microscopes.

Tube formation assay. Ninety-six-well plates were coated with Growth-Factor-Reduced Matrigel (BD Biosciences) mixed with rat neutralizing-antibody against human CCR3 (20 μg ml^{-1}, R&D Systems) or control rat IgG2a (Invitrogen) and allowed to solidify in the incubator at 37 °C for 45 min. Human CECs[44–47] were plated on top of the Matrigel at 2.25×10^4 cm^{-2} in EBM-2 basal media (Cambrex) containing 1% FBS with CCR3 antibody or rat IgG2a at the concentrations shown and allowed to grow overnight. Tube formation was analysed by counting the number of cell junctions per mm^2.

Proliferation assay. Human CECs were synchronized for cell cycle state by first cultivating them in EGM2-MV media (Lonza) supplemented with 10% FBS (Gibco) to achieve complete confluence, and then by overnight serum starvation in MCDB131 media (Gibco) with 0.1% FBS. They were passaged to 96-well plates at a density of 5,000 cells per well, followed by stimulation for 24 h with eotaxin-1, 2 or 3 (10 ng, 100 ng and 2 μg per ml, respectively; Peprotech) in MCDB131 media with 0.1% FBS. After 24 h, cell viability was measured with BrdU ELISA (Chemicon) according to the manufacturer's instructions.

F-actin polymerization assay. Human CECs were seeded in black-walled 96-well plates and grown to 70–80% confluence in fully supplemented EGM-2MV. Cultures were serum-starved overnight in basal media and then stimulated with recombinant human eotaxin-1 (10 ng ml^{-1}), eotaxin-2 (100 ng ml^{-1}), eotaxin-3 (2 μg ml^{-1}) (Peprotech), or vehicle control (PBS). At 0, 10, 30, 60 or 120 s timepoints, cells were fixed in 3.7% paraformaldehyde for 10 min, washed, permeabilized in PBS with 0.1% Triton X-100, and then stained with rhodamine-labelled phalloidin (1:200, Invitrogen) as per the manufacturer's recommendations. Plates were analysed on a fluorescent plate reader (Synergy 4, Biotek) followed by fluorescent microscopy (Nikon E800).

Migration assay. Eotaxins-1, -2 and -3 were reconstituted in 0.1% BSA and then mixed with Matrigel diluted 1:1 with serum-free endothelial basal media (EBM-2; Lanza). Five-hundred microlitres of EBM-2 was added to each well of a 24-well plate, followed by a 6.5-mm diameter Transwell insert (8 μm pores; Corning). Human CECs in EBM-2 were prestained with Vybrant DiO (Invitrogen) for 30 min at 37 °C and seeded into the inserts at 50,000 cells per 200 μl of serum free EBM-2 media. The plates were allowed to incubate for 16 h at 37 °C, 5% CO_2. The migrated cells were imaged with an Olympus CK40 microscope and Olympus DP71 camera.

RAC1 activation. Human CECs were cultured in EGM-2 MV containing 5% FBS. Before starting the assay, cells were serum-starved overnight using basal medium (MCDB131) supplemented with 1% FBS. Cells were stimulated for designated times with eotaxin-1, -2 and -3 (10 ng ml^{-1}, 100 ng ml^{-1} and 2 μg ml^{-1}, respectively). Equal amounts of lysates (500 μg) were incubated with GST–Pak1–PBD agarose beads (Upstate) to pull down active GTP-bound RAC1 at 4 °C for 1 h with rotation. The samples were subsequently analysed for bound RAC1 by western blot analysis using an anti-RAC1 antibody (Upstate).

Electroretinography. Mice were dark-adapted overnight and then anaesthetized. Both eyes were positioned within a ColourBurst Ganzfeld stimulator (Diagnosys). Espion software (Diagnosys) was used to program a fully automated flash intensity series, from which retinal responses were recorded.

44. Geisen, P., McColm, J. R. & Hartnett, M. E. Choroidal endothelial cells transmigrate across the retinal pigment epithelium but do not proliferate in response to soluble vascular endothelial growth factor. *Exp. Eye Res.* **82**, 608–619 (2006).
45. Peterson, L. J., Wittchen, E. S., Geisen, P., Burridge, K. & Hartnett, M. E. Heterotypic RPE-choroidal endothelial cell contact increases choroidal endothelial cell transmigration via PI 3-kinase and Rac1. *Exp. Eye Res.* **84**, 737–744 (2007).
46. Smith, J. R. *et al.* Unique gene expression profiles of donor-matched human retinal and choroidal vascular endothelial cells. *Invest. Ophthalmol. Vis. Sci.* **48**, 2676–2684 (2007).
47. Zamora, D. O. *et al.* Proteomic profiling of human retinal and choroidal endothelial cells reveals molecular heterogeneity related to tissue of origin. *Mol. Vis.* **13**, 2058–2065 (2007).